MOLECULAR PHYSICS, 2002, VOL. 100, NO. 16, 2653–2658

Taylor & Francis
Taylor & Francis Group

Ab initio and RRKM studies of decomposition and interconversion pathways of $ClCH_2OH$ and CH_3OCl isomeric species

EVANGELOS DROUGAS[1], AGNIE M. KOSMAS[1*], MELANIE SCHNELL[2], MAX MÜHLHÄUSER[2] and SIGRID D. PEYERIMHOFF[2]

[1]Department of Chemistry, University of Ioannina, 451 10, Greece
[2]Institut für Physicalische und Theoretische Chemie der Universität Bonn, Wegelerstrasse 12, 53115 Bonn, Germany

(*Received 14 January 2002; accepted 28 February 2002*)

The photofragmentation and photointerconversion pathways of the CH_3OCl and $ClCH_2OH$ species are studied using quantum mechanical and RRKM theories. Ten possible channels are investigated in total and the relative importance of the various pathways in stratospheric photochemistry is discussed.

1. Introduction

The well established involvement of chlorinated hydrocarbons in the stratospheric ozone chemistry [1–4] has led to the investigation of many chlorinated species that may act as chlorine reservoirs [5, 6] or interfere in other ways in the catalytic ozone depletion cycles. Methyl hypochlorite is such a compound, well studied both experimentally [7–9] and theoretically [10–14], as has its isomeric species chloromethanol [15]. Recently, Li and Francisco [16] and Schnell *et al.* [17] studied the low lying electronic states of CH_3OCl and $ClCH_2OH$, respectively, and investigated the potential energy surfaces for the most important photofragmentation routes for these two systems. For CH_3OCl the lowest lying excited potential energy curves along the Cl–O coordinate were found to be highly repulsive, while all the corresponding excited potential energy curves along the C–O coordinate were found to contain energetic minima. Thus, it was concluded that the photodissociation pathways of CH_3OCl should proceed along the strongly repulsive O–Cl rather than the C–O coordinate. For $ClCH_2OH$ the lowest lying excited potential energy curves were found to be highly repulsive along the C–Cl coordinate while photodissociation along the C–O direction has to overcome a barrier of about 0.3 eV. Other recent *ab initio* studies have been devoted to an examination of CH_3OCl decomposition channels [18] and the relevant investigation of the mechanism of the CH_3+ClO reaction [19]. Finally, Drougas *et al.* [20], using variational RRKM theory, calculated bimolecular rate coefficients at 298 K for the two most important channels of the reaction between methyl radicals and chlorine monoxide, leading to the products CH_3O+Cl and HCHO+HCl through the intermediate formation of CH_3OCl. The extensive theoretical investigations underline the particular interest associated with the various photofragmentation pathways of the $ClCH_2OH$ and CH_3OCl isomeric forms.

We present a kinetic study of the decomposition and interconversion pathways of the ground state CH_3OCl and $ClCH_2OH$ species. The following reaction channels are considered.

A. Production pathways for methyl hypochlorite

$$CH_3OCl \rightarrow CH_3 + OCl \quad (1)$$

$$CH_3OCl \rightarrow CH_3O + Cl \quad (2)$$

$$CH_3OCl \rightarrow CH_2 + HOCl \quad (3)$$

$$CH_3OCl \rightarrow cis\text{-}HCOCl + H_2 \quad (4)$$

$$CH_3OCl \rightarrow HCHO + HCl \quad (5)$$

$$CH_3OCl \rightarrow ClCH_2OH \quad (6)$$

B. Production pathways for chloromethanol

$$ClCH_2OH \rightarrow Cl + CH_2OH \quad (7)$$

$$ClCH_2OH \rightarrow ClCH_2 + OH \quad (8)$$

$$ClCH_2OH \rightarrow HCHO + HCl \quad (9)$$

$$ClCH_2OH \rightarrow CH_3OCl \quad (10)$$

Energy-specific microcanonical rate constants $k(E)$ were calculated for processes (1)–(10) with the main issue being the evaluation of the relative importance of each production channel to the overall kinetics of

* Author for correspondence. e-mail: amyloma@cc.uoi.gr

Molecular Physics ISSN 0026–8976 print/ISSN 1362–3028 online © 2002 Taylor & Francis Ltd
http://www.tandf.co.uk/journals
DOI: 10.1080/00268970210137293

each system and the mechanism of each reaction, including bond scission, four-centre elimination and interisomerization.

2. Quantum mechanical calculations and results

Geometry optimizations of all the species involved in steps (1)–(10) were performed with large scale singles and doubles coupled cluster calculations with perturbative inclusion of connected triple excitations (CCSD(T)), using the polarized triple-zeta cc-p-VTZ basis sets from Dunning [21]. This is a higher level of theory employed than in previous calculations [18–20]. The Molpro 2000 program package was used [22]. Well defined, tight transition states were determined in production channels (4), (5), (6), (9) and (10) and they have been labelled according to the corresponding channel as TS4, TS5, TS6,10 and TS9. The optimized structures for the two isomeric minima and the transition states are depicted in figure 1 and generally they agree well with what could be deduced from the literature. For example, in $ClCH_2OH$ we obtained 1.395 Å and 1.787 Å for the CO and CCl bond lengths, respectively, which are in line with the corresponding 1.385 Å and 1.797 Å values calculated at the MP2/6-311++G(d, p) level [19]. The CO and OCl bonds in CH_3OCl were calculated as 1.425 Å and 1.689 Å, respectively, comparing well with 1.425 Å and 1.709 Å at the CCSD(T)/6-311G(2df, 2p) level [12].

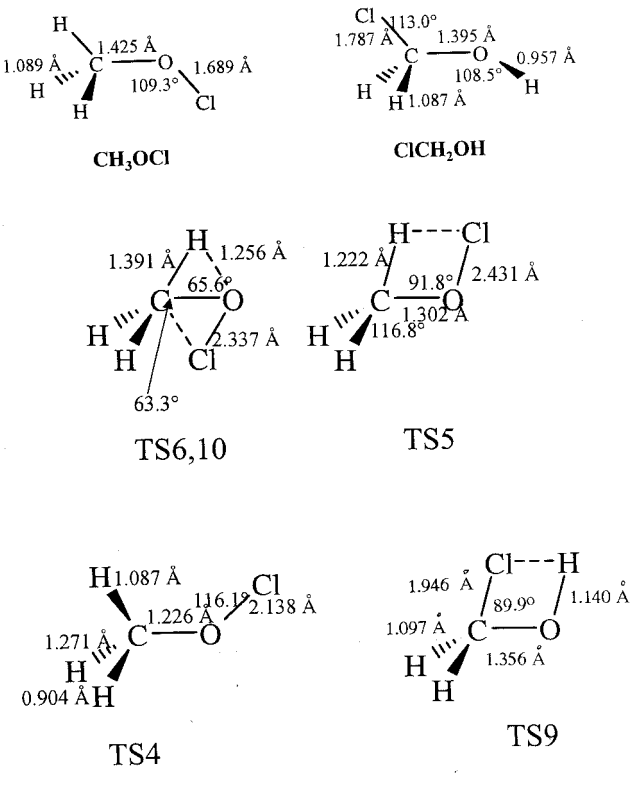

Figure 1. Optimized structures for stationary points of CH_3OCl and $ClCH_2OH$ production pathways.

The structures for the various transition states are also in reasonable agreement with what is known from the literature [18–20]. For example, the CO bond distance and HCO angle in TS5 that leads to HCHO + HCl from CH_3OCl were found to be 1.302 Å and 91.8°, comparing very well with the corresponding values of 1.304 Å and 97.7° by He *et al.* [18]. The ClO bond distance in TS6,10 for the interisomerization process was found to be 2.337 Å, comparing well with 2.314 Å by Zhou *et al.* [19]. The transition states have been characterized by vibrational analysis as first-order saddle points possessing one imaginary frequency, while the optimized structures for the minima present exclusively positive frequencies. Finally, the optimized structures for the reaction products are also in very good agreement with analogous results in the literature [16–20], and for this reason they are not included in figure 1.

Vibrational frequencies and moments of inertia calculated at the B3LYP and MP2 levels of theory, using the Gaussian98 series of programs [23], are collected in table 1. The calculated IR frequencies of the stationary points are in reasonable agreement with experimental and other theoretical data [18–20, 30, 31]. For example, in $ClCH_2OH$ we assigned the C–O stretch with 1083 cm^{-1}, the OH stretch with 3545 cm^{-1} and the OH torsion with 331 cm^{-1}, in good agreement with the experimental values of Wallington *et al.* [30] and Kunttu *et al.* [31].

Decomposition channels (1), (2), (3), (7) and (8) occur without a distinct energy barrier, i.e. they are simple bond fission processes. For each of these pathways a number of energy points at the MP2(full)/6-31++G(3df, 3dp) level of theory were examined in the exit valley of the potential surface. These points were investigated by varying the reaction coordinate from the energy minimum outwards and allowing full optimization of the remaining structural parameters of the system. From this series of points for each production pathway, one was selected in each case, which shows the minimum number of energy states for use in the kinetic calculations [24]. The properties of these reaction points (denoted hereafter as RP*j*, i.e. labelled after the corresponding channel as RP1, RP2, RP3, RP7 and RP8) are also included in table 1. All the RP*j* points selected were found located at a near-zero energy difference with respect to the corresponding products.

Figure 2 presents a reaction energy profile based on coupled cluster (CCSD(T)) calculations. Chloromethanol, $ClCH_2OH$, is about 40 kcal mol^{-1} lower in energy than isomeric methylhypochlorite, CH_3OCl. The two isomers are separated by a transition state (TS6,10 in figure 2) resulting in a barrier of 66 kcal mol^{-1} relative

Table 1. *Ab initio* harmonic vibrational frequencies (in cm^{-1}) and moments of inertia (in au) for energy minima, transition states and reaction points involved in processes (1)–(10).

Species	Frequencies	I_a	I_b	I_c
CH_3OCl	3133, 3113, 3038, 1537, 1488, 1475, 1204, 1181, 1020, 661, 365, 261	43.0	297.5	328.9
$ClCH_2OH$	3545, 3034, 2934, 1456, 1353, 1297, 1150, 1083, 926, 615, 442, 231	45.9	330.8	360.5
TS6,10	3213, 3093, 1850, 1543, 1334, 1193, 1073, 824, 458, 342, 124, 1800i	57.9	353.1	398.0
TS4	3218, 2545, 1739, 1460, 1293, 1120, 899, 844, 385, 306, 241, 1339i	44.5	402.7	426.2
TS5	3046, 2956, 1736, 1531, 1261, 1243, 1179, 957, 502, 398, 302, 1891i	52.3	389.7	433.2
TS9	3779, 3132, 3051, 1554, 1418, 1275, 1256, 1093, 1008, 670, 380, 487i	47.0	320.6	356.1
RP1	3354, 3354, 3161, 1464, 1463, 985, 788, 584, 547, 209, 64, 273i	73.2	443.8	503.9
RP2	3095, 3048, 2961, 1552, 1443, 1407, 1189, 1172, 1018, 228, 221, 230i	50.7	518.9	525.4
RP3	3342, 3009, 2897, 2829, 1405, 1373, 1365, 1223, 1112, 1011, 810, 716i	18.9	461.0	482.5
RP7	3505, 3034, 2934, 1456, 1353, 1297, 1150, 1083, 626, 415, 342, 223i	33.9	216.9	247.3
RP8	3445, 3167, 3276, 1499, 1238, 1091, 1074, 841, 668, 510, 384, 541i	24.7	413.5	436.4

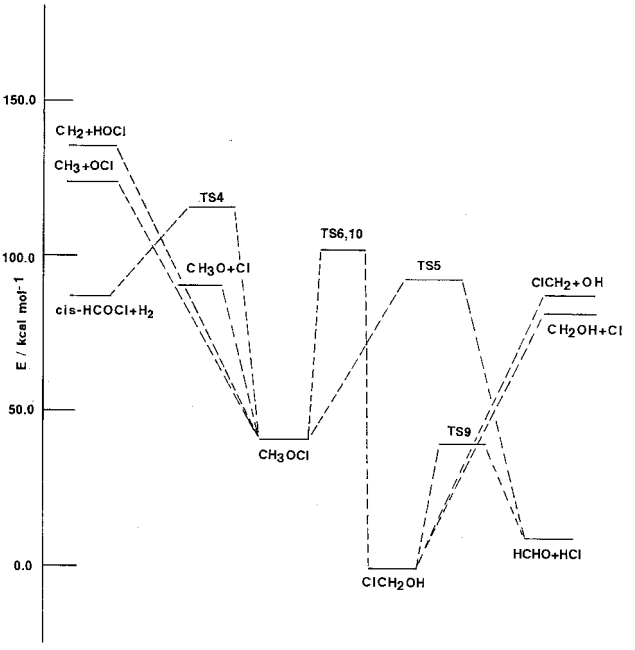

Figure 2. Energy profile of CH_3OCl and $ClCH_2OH$ production pathways.

to CH_3OCl in channels (6) and (10). This value is in good agreement with the barrier height of 62.7 kcal mol^{-1} calculated by He *et al.* [18] at the G2MP2 level. One important reaction scheme is the unimolecular decomposition forming HCHO+HCl via a 1,2 HCl elimination out of each isomer, channels (5) and (9). The products HCHO and HCl are about 10.2 kcal mol^{-1} higher in energy than $ClCH_2OH$, and consequently about 31.7 kcal mol^{-1} lower in energy relative to CH_3OCl. The transition state for the decomposition of $ClCH_2OH$ into HCHO + HCl, channel (9), leads to an energy barrier of about 53 kcal mol^{-1} relative to $ClCH_2OH$ with an imaginary frequency of 487 cm^{-1} and elongated CCl and OH distances. Zhou *et al.* [19] obtained a corresponding barrier of 40.8 kcal mol^{-1} and an imaginary frequency of 646 cm^{-1} at the G2MP2/6-311(d,p) level. The 1,2 HCl elimination from CH_3OCl, channel (5), is also hindered by a barrier of 55 kcal mol^{-1}, which compares well with the value of 53.1 kcal mol^{-1} obtained by He *et al.* [18]. Another interesting reaction path is the 1,1-α elimination of H_2, channel (4), leading to *cis*-HCOCl. The reaction mechanism can be described by the elongation of two CH bonds with a simultaneous abridgment of the distance between the appendant hydrogen centres. In the transition state TS4 the two breaking CH bonds are 1.271 Å and 1.490 Å, considerably longer than in CH_3OCl, and the forming HH bond is 0.904 Å. The calculated barrier height is 79 kcal mol^{-1} with an imaginary frequency of 1339 cm^{-1}, compared with 71.2 kcal mol^{-1} and 2869 cm^{-1}, respectively, computed by He *et al.* [18].

The other three decomposition channels, (1), (2) and (3), occur without a distinct energy barrier. Reactions (1) and (2) are simply cleavage reactions of CO and OCl bonds, respectively, and they are endothermic by 79.3 kcal mol^{-1} and 47.4 kcal mol^{-1}. The third reaction (3) can be described as an H migration mechanism with an endothermicity of 93 kcal mol^{-1}. Our values are in reasonable agreement with the corresponding values 50.5, 78.1 and 89.6 kcal mol^{-1} of He *et al.* [18]. Finally, to complete the present study of $ClCH_2OH$ decomposition the two new reaction steps (7) and (8) were examined. These channels are also described as simple fissions of C-Cl and C-O bonds, presenting the high endo-

thermicities of $80.5\,\mathrm{kcal\,mol^{-1}}$ and $95.4\,\mathrm{kcal\,mol^{-1}}$, respectively.

3. RRKM calculations

The energy specific microcanonical rate constants $k(E)$ for the reaction channels (1)–(10) were evaluated using the RRKM (Rice–Ramsperger–Kassel–Marcus) theory [25]. For a given reaction step at an initial reactant energy $E, k_i(E)$ is given by

$$k_i(E,J) = W_i(E,J)/h\varrho_M(E,J), \qquad (11)$$

where $\varrho_M(E,J)$ is the density of states available to the minimum at a reactant energy E and $W_i(E_i,J)$ is the number of states for the active degrees of freedom of the transition state TS_i being involved in the considered reaction step $i = 1,\ldots,10$. The calculations have been carried out employing the corresponding algorithm [26]. The required input consists of the harmonic frequencies and the moments of inertia and it is summarized in table 1. RRKM theory was directly applied to processes (4), (5), (6), (9) and (10), which were found to proceed through the tight transition state configurations, TS4, TS5, TS6,10 and TS9. Processes (1), (2), (3), (7) and (8) were found to proceed via barrierless decomposition pathways, as described in the previous section. To apply the RRKM methodology for the examination of these channels the principles of variational RRKM theory were employed. According to variational theory, the bottleneck of a reaction occurs at the point along the minimum energy path where the number of states available, and hence the microcanonical rate constant, is at a minimum [24–29]. Consequently, calculations were performed at calculated reaction points along the minimum energy path for each production pathway until a minimum in the rate was found, thereby defining the reaction bottleneck. As in several previous variational RRKM calculations for radical–molecule and radical–radical barrierless association and decomposition reactions [20, 28, 29] we have found that the minimum in the rate occurs at a reaction point RPj along the minimum energy path that is located at a near zero energy difference with respect to products. The variational evaluation of the rate coefficient for each channel produced a minimum value at the selected reaction points, i.e. at RP1, RP2, RP3, RP7 and RP8 located at the exit valley of each of the pathways under consideration and at a zero energy difference with respect to the separating fragments. Their molecular properties have been used in the RRKM calculations.

4. Results and discussion

Figures 3 and 4 present the microcanonical rate constants for the CH_3OCl and $ClCH_2OH$ production channels, respectively. We first discuss the reaction pathways of the CH_3OCl system. For an accurate treatment, the reverse process of isomerization reaction (10) and decomposition reactions (7)–(9) of chloromethanol should be taken into account. However, as we can see, these channels appear to be unimportant with regard to the CH_3OCl system because they present reaction rates much lower compared with the CH_3OCl decomposition channels, as a result of the greater stability of chloromethanol. The most important production pathways resulting from the photoactivation of CH_3OCl system are the OCl bond scission to form the $CH_3O + Cl$ products, reaction (2), the 4-centre elimination to HCHO+HCl, reaction (5), and the isomerization to chloromethanol, $ClCH_2OH$, reaction (6), $k_2 > k_5 > k_6$, in accordance with the order of the activation barriers that have to be overcome in each channel. The values of the calculated rates are quite significant well below $100\,\mathrm{kcal\,mol^{-1}}$ where photoexcitation of CH_3OCl begins to occur [16], and hence these processes must be important production channels of methyl hypochlorite in stratospheric photochemistry. Step (1) leading to CO bond scission, $CH_3 + OCl$, and step (4)

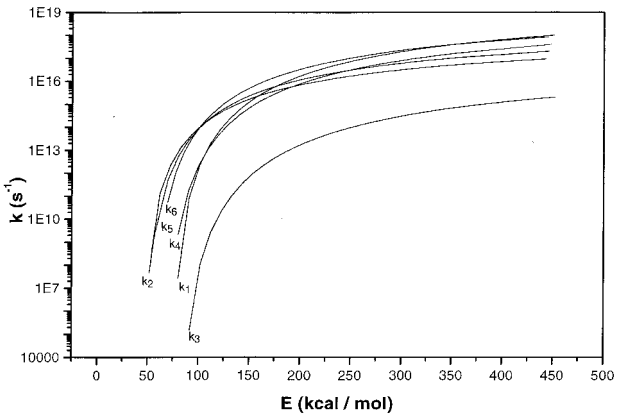

Figure 3. Microscopic rate constants for channels (1)–(6).

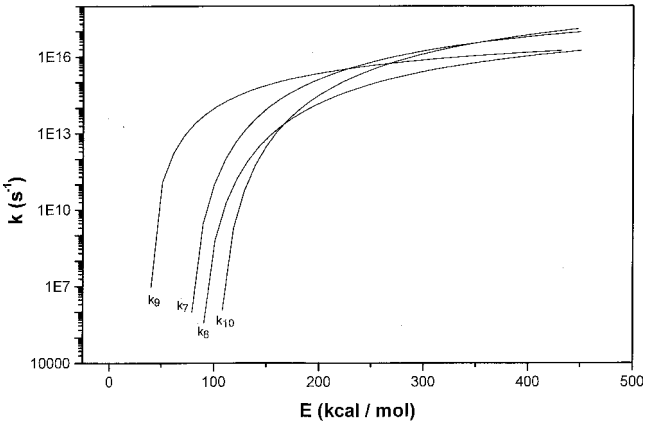

Figure 4. Microscopic rate constants for channels (7)–(10).

leading to H_2 formation, H_2 + *cis*-HCOCl, follow afterwards, since they exhibit higher activation energy barriers but they rise fast. Above 150 kcal mol^{-1} all production channels except path (3) become important and begin to compete with each other, with channel (1) gaining greatly in significance among the others. This is expected because the low frequencies of reaction point RP1 are much lower than the low frequencies of the competing channels. The less significant pathway in the CH_3OCl system is the H atom migration to Cl leading to the products HOCl+CH_2, which remains much lower throughout the entire interesting energy region.

In the case of $ClCH_2OH$ photofragmentation the situation is more distinct. The important observation is the much lower $k(E)$ values by about an order of magnitude for all production pathways of $ClCH_2OH$ compared with the CH_3OCl isomer, reflecting the much higher stability of the $ClCH_2OH$ molecule. At a high energy, $E = 400$ kcal mol^{-1}, the $k(E)$ values for the most important pathways of CH_3OCl system reach the order of 10^{18} s^{-1}, while the most important channels for $ClCH_2OH$ just reach the order of 5×10^{16} s^{-1}. Another interesting feature is the different rates of isomerization. The CH_3OCl isomerization to $ClCH_2OH$ at $E = 125$ kcal mol^{-1} takes place with a rate constant of the order of 3×10^{15} s^{-1} while the reverse process $ClCH_2OH \rightarrow CH_3OCl$ presents a rate constant of about 5×10^{10} s^{-1}. Hence, photoactivation of CH_3OCl will produce chloromethanol as one of the major channels, which is not the case for the opposite direction. Indeed, photoisomerization of $ClCH_2OH$ to CH_3OCl appears to be the least probable reaction pathway for the fate of chloromethanol under photoactivation at low energies, lower than 150 kcal mol^{-1} where photoexcitation of this molecule begins to take place [17]. This is a direct consequence of the order of the activation energy barriers that have to be overcome in each case. The isomerization rate rises fast, however, and crosses the other rates, becoming an important channel above 200 kcal mol^{-1}, again as a result of the lower values of the low frequencies. Thus, the ClC and CO bond scissions in $ClCH_2OH$ appear more probable than isomerization at low energies, although the most significant channel in the low energy region is the 4-centre elimination to HCHO+ HCl. Nevertheless, as already said, this order changes quickly with increasing energy, and the isomerization rate rises quickly, surpassing the 4-centre elimination process and competing with the ClC bond scission pathway.

A comparison of processes (5) and (9) is interesting since they both lead to the same 4-centre 1,2 elimination products HCHO + HCl starting from the corresponding *cis* conformation of each isomer. At $E = 75$ kcal mol^{-1} process (5) occurs with a rate of the order of 4×10^{12} s^{-1} while process (9) appears faster with a reaction rate of about 2×10^{13} s^{-1}. However, k_5 increases more quickly and both rates rise to large values of about 10^{15} s^{-1} when the energy doubles at 150 kcal mol^{-1}.

To summarize the results of the present study we may conclude that both isomers $ClCH_2OH$ and CH_3OCl, although kinetically stable under thermal energy conditions [5], present important photolytic dissociation and interisomerization pathways under photoactivation at energies lower than that at which excitation to higher electronic states occurs. These pathways are expected to play an interesting part in the overall stratospheric photochemistry of chlorine containing compounds.

The present study is part of a NATO science project 'Study of elementary steps of radical reactions in atmospheric chemistry'. Financial support from the NATO collaborative linkage, Grant EST.CLG.977083, is gratefully acknowledged.

References

[1] Farman, J. C., Gardiner, B. G., and Shankin, J. D., 1985, *Nature*, **315,** 207.
[2] Simone, F. G., Burrows, J. P., Schneider, W., Moortgat, G. K., and Crutzen, P. J., 1989, *J. phys. Chem.*, **93,** 7808.
[3] Solomon, S., 1990, *Nature*, **347,** 347.
[4] Anderson, J. G., Tooley, D. W., and Brune, W. H., 1991, *Science*, **251,** 39.
[5] Helleis, F., Crowley, J. N., and Moortgat, G. K., 1993, *J. phys. Chem.*, **97,** 11464.
[6] Crowley, J. N., Campuzano-Jost, P., and Moortgat, G. K., 1996, *J. phys. Chem.*, **100,** 3601.
[7] Rigden, J. S., and Butcher, S. S., 1964, *J. chem. Phys.*, **40,** 2109.
[8] Crowley, J. N., Helleis, F., Muller, R., Moortat, G. K., Crutzen, P. J., and Orlando, J. J., 1994, *J. geophys. Res.*, **99,** 20683.
[9] Jung Kamp, T. P.W., Kirchner, U., Schmidt, M., and Schindler, R. N., 1995, *J. Photochem. Photobiol.* A, **91,** 1.
[10] Messer, B. M., and Elrod, M. J., 1999, *Chem. Phys. Lett.*, **301,** 10.
[11] Espinosa-Garcia, J., 1999, *Chem. Phys. Lett.*, **315,** 239.
[12] Francisco, J. S., 1999, *Intl. J. Quantum Chem.*, **73,** 29.
[13] Espinosa-Garcia, J., 2000, *Chem. Phys. Lett.*, **316,** 563.
[14] Jung, D., Chen, C.-J., and Bozzelli, J. W., 2000, *J. phys. Chem.* A, **104,** 9581.
[15] Muhlhauser, M., Schnell, M., and Peyerimhoff, S. D., 2002, *Molec. Phys.*, in press.
[16] Li, Y., and Francisco, J. S., 1999, *J. chem. Phys.*, **111,** 8384.
[17] Schnell, M., Muhlhauser, M., and Peyerimhoff, S. D., 2001, *Chem. Phys. Lett.*, **344,** 519.
[18] He, T.-J., Chen, D.-M., Liu, F.-C., and Sheng, L.-S., 2000, *Chem. Phys. Lett.*, **332,** 545.
[19] Zhou, X., Li, J., Zhao, X., Tian, Y., Zhang, L., Chen, Y., Chen, C., Yu, S., and Ma, X., 2001, *Phys. Chem. chem. Phys.*, **3,** 3662.

[20] Drougas, E., Papayannis, D. K., and Kosmas, A. M. 2002, *Chem. Phys.*, **276,** 15.
[21] Poirierer, R., Kari, R., and Csimadia, I., 1985, *Handbook of Gaussian Basis Sets* (Amsterdam: Elsevier) p. 225 (Nr. 6.59.4).
[22] Werner, H. J., and Knowles, P. J., Molpro 2000, a package of *ab initio* programs.
[23] Frish, M. J., Trucks, G. W., Schlegel, H. B. *et al.*, 1998, Gaussian98, Revision A.7 (Pittsburgh, P.A: Gaussian Inc.).
[24] Klippenstein, S. J., 1992, *J. chem. Phys.*, **96,** 367.
[25] Baer, T., and Hase, W. L., 1996, *Unimolecular Reaction Dynamics* (Oxford University Press).
[26] Zhu, L., and Hase, W. L., QCPE 644.
[27] Liu, Y.-P., Lu, D.-H., Gonzalez-Lafont, A., Truhlar, D. G., and Garrett, B. C., 1993, *J. Amer. chem. Soc.*, **115,** 7806.
[28] Guadagnini, R., Schatz, G. C., and Walch, S. P., 1998, *J. phys. Chem.* A, **102,** 5857.
[29] Simonson, M., Bradley, K. S., and Schatz, G. C., 1995, *Chem. Phys. Lett.*, **244**, 19.